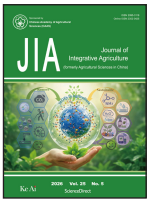
Journal of Integrative Agriculture 2026, 25(5): 1949–1960

Available online at ScienceDirect

Journal of Integrative Agriculture



RESEARCH ARTICLE

Transcriptomic and metabolomic analyses reveal the mechanism of anthocyanin metabolism in H18 pepper leaves and the function of *CaDFR1*

Han Wang[1, 2, 3*], Dongchen Li[4*], Congsheng Yan[1, 2, 3], Muhammad Aamir Manzoor[5], Qiangqiang Ding[1, 2, 3], Yan Wang[1, 2, 3], Xiujing Hong[1, 2, 3], Tingting Song[1, 2, 3], Li Jia[1, 2, 3#], Haikun Jiang[1, 2, 3#]

[1] *Institute of Vegetables, Anhui Academy of Agricultural Sciences, Hefei 230001, China*
[2] *Key Laboratory of Horticultural Crop Germplasm Innovation and Utilization (Co-construction by Ministry and Province), Hefei 230001, China*
[3] *Anhui Provincial Key Laboratory for Germplasm Resources Creation and High-Efficiency Cultivation of Horticultural Crops, Hefei 230001, China*
[4] *College of Life Sciences, Anhui Agricultural University, Hefei 230036, China*
[5] *School of Agriculture and Biology, Shanghai Jiao Tong University, Shanghai 200030, China*

Highlights

- The accumulation of anthocyanins in H18 pepper plants leads to purple leaves, and the anthocyanin content in leaves decreases with plant growth and development.
- Anthocyanins produced with dihydromyricetin (DHM) as substrate are the main component of anthocyanins in H18 pepper leaves.
- CaDFR1 plays an important role in the anthocyanin synthesis pathway of pepper leaves.

Abstract

Anthocyanins play a crucial role in plant growth, development, reproduction, and stress response. Additionally, anthocyanins enhance the quality of fruits and vegetables due to their antioxidant properties. While numerous previous studies have been conducted on anthocyanins, limited information exists regarding their composition and the role of the anthocyanin pathway gene dihydroflavonol 4-reductase (*DFR*) in chili pepper leaves. In this study, we used a purple leaf pepper cultivar H18 in which the anthocyanin content in leaves decreases with plant growth and development. Targeted anthocyanin metabolite assays revealed that the contents of delphinidin, malvidin, and petunidin derivatives followed the same trend as the overall anthocyanin content, with delphinidin derivatives being the predominant component of H18 pepper leaves. Transcriptome sequencing was performed on H18 leaves at four different stages. The results showed that differentially expressed genes (DEGs) at various stages were primarily associated with biological processes and flavonoid metabolic pathways. Through phylogenetic tree and expression analysis, we identified three candidate genes involved in DFR function. Substrate catalysis assays of CaDFRs demonstrated that only CaDFR1 was active, catalyzing dihydroquercetin (DHQ), dihydromyricetin (DHM), and dihydrokaempferol (DHK). VIGS-mediated silencing of *CaDFR1* resulted in a significant decrease in anthocyanin levels in H18 pepper leaves and stems, along with a reduction in the expression levels of other candidate functional genes in the anthocyanin metabolic pathway. This study identifies the key anthocyanin components in the leaves of H18 peppers and validates the function of CaDFR1, providing a theoretical foundation for modifying anthocyanin content in pepper plants through molecular breeding.

Keywords: anthocyanins, transcriptomic and metabolomic, dihydroflavonol 4-reductase, functional validation

1. Introduction

In nature, plant organs are colored by various pigments, including chlorophyll, anthocyanins, carotenoids, and betalains (Cackett *et al.* 2022; Kapoor *et al.* 2022; Rodríguez-

Received 13 February 2025; Received in revised form 20 June 2025; Accepted 25 September 2025; Available online 22 October 2025
[#]Correspondence Haikun Jiang, Tel/Fax: +86-551-65160817, E-mail: Jhk211@163.com; Li Jia, Tel/Fax: +86-551-65160817, E-mail: jiali820@aaas.org.cn
[*] These authors contributed equally to this study.

© 2026 CAAS. Publishing services by Elsevier B.V. on behalf of KeAi Communications Co. Ltd. This is an open access article under the CC BY-NC-ND license (http://creativecommons.org/licenses/by-nc-nd/4.0/). Peer review under responsibility of Editorial Board of *Journal of Integrative Agriculture*.
doi: 10.1016/j.jia.2025.10.011

Mena *et al.* 2023). Plant pigments play essential roles in various plant processes, including photosynthesis, defense, and reproduction (Xia *et al.* 2021; Davies *et al.* 2022; Li *et al.* 2022). Among these, anthocyanins are of particular significance due to their antioxidant properties, which help maintain reactive oxygen species (ROS) homeostasis in plant cells (Cerqueira *et al.* 2023). Furthermore, anthocyanins act as natural "sunscreen," mitigating damage caused by ultraviolet radiation under intense sunlight (Espley and Jaakola 2023; Shi *et al.* 2023). In addition to their role in stress response, anthocyanins have beneficial effects on human health (Petroni *et al.* 2014). Recent studies also suggest that anthocyanins can serve as markers to identify male sterile and fertile strains in male sterility breeding (Du *et al.* 2020).

The anthocyanin biosynthetic pathway has been extensively characterized and validated (Saigo *et al.* 2020). Anthocyanins are derived from the phenylpropane metabolic pathway, which is involved in flavonoid synthesis. The precursors for anthocyanin biosynthesis include malonyl CoA and *p*-coumaroyl CoA (Zhang *et al.* 2014). Malonyl CoA and *p*-coumaroyl CoA are catalyzed by chalcone synthase (CHS) and chalcone isomerase (CHI) to form the colorless naringenin (Araguirang and Richter 2022). Naringenin is subsequently converted into dihydrokaempferol (DHK) by F3H. DHK can be further catalyzed by F3′H and F3′5′H to form dihydroquercetin (DHQ) and dihydromyricetin (DHM) (Katsu *et al.* 2017). The colorless DHK, DHQ, and DHM are further reduced to unstable leucoanthocyanidin by dihydroflavonol 4-reductase (DFR), which are then synthesized into six major anthocyanins: cyanidin, peonidin, delphinidin, petunidin, malvidin, and pelargonidin by anthocyanin synthase (ANS) and flavonoid 3-*O*-glucosyltransferase (3GT) (Liu *et al.* 2020; Rodríguez-Mena *et al.* 2023; Ying *et al.* 2024). DFR is the first enzyme in this pathway that belongs to the NADPH-dependent epimerase/dehydratase family and is crucial for converting dihydroflavonols to anthocyanosides (Petit *et al.* 2007). The role of DFR in anthocyanin synthesis is regulated by the MYB-bHLH-WD40 (MBW) complex (Koes *et al.* 2005; Tian *et al.* 2017). Due to the distinct substrate selectivity of DFRs across species, plants can produce a diverse range of anthocyanins, resulting in a wide spectrum of colors. Studies have shown that DFR is closely linked to the color of petals and seed coats. For instance, the *Arabidopsis* DFR-deficient mutant *tt3* exhibits a complete absence of proanthocyanidin (PA) accumulation, resulting in a transparent seed coat (Kubasek *et al.* 1992; Bharti and Khurana 2003). Similarly, DFR-deficient gerberas (*Gerbera hybrida*) display white petals (Bashandy *et al.* 2015). Additionally, the *CsDFRa* and *CsDFRc* genes from tea have been shown to be involved in anthocyanin and PAs biosynthesis (Ruan *et al.* 2022). The identification of two anthocyanin-free mutants in eggplant (*Solanum melongena*) was confirmed to be due to a mutation in the 50 splice sites of the second intron of the eggplant *DFR* gene (Wang *et al.* 2022).

Pepper (*Capsicum annuum* L.), a member of the Solanaceae family, is a highly important vegetable crop, with its cultivation area ranking first among vegetable crops in China. It also exhibits significant hybrid advantages (Baenas *et al.* 2019; Zhang *et al.* 2022; Fang *et al.* 2025). Anthocyanin-rich pepper plants are known for their combined resistance to heat, drought, and viral diseases (Wang *et al.* 2018). To meet the varying demands of pepper plants across different regions and under different growing conditions, it is essential to breed diverse pepper varieties, particularly those rich in anthocyanins and possessing higher resistance. In this study, we developed the purple-leaved and colorful-fruited self-stabilized pepper variety H18 through variety-directed selection. We observed that the leaves of H18 plants gradually turned green during development. We sequenced the transcriptomic and metabolomic of H18 leaves at four developmental stages, conducting a joint analysis to identify functional genes in the *DFR* gene family involved in anthocyanin metabolism. This research explores key functional genes in anthocyanin synthesis and validates the role of DFR, providing a theoretical foundation for the molecular breeding of anthocyanin-enhanced chili peppers.

2. Materials and methods

2.1. Plant materials

In this study, we developed the purple-leaved and colorful-fruited self-stabilized pepper variety H18 (*C. annuum* L.) through variety-directed selection at the Vegetable Research Institute of the Anhui Academy of Agricultural Sciences, China. The plants were cultivated in a constant temperature laboratory incubator (20–25°C in 16 h/8 h light/dark cycles with 60% relative humidity). Leaves were sampled at different development stages; the purple of cotyledon stage (5 days after germination, S1), the purple of true leaves stage (12 days after germination, S2), the fading purple color of the true leaves stage (20 days after germination, S3), and the green of true leaves stage (30 days after germination, S4). Samples from each stage were divided into three replicates, rapidly cooled in liquid nitrogen, and then stored at –80°C and experimental analysis.

2.2. Detection of anthocyanins

Anthocyanin extraction was performed according to methods referenced from previous studies with minor modifications (Ruan *et al.* 2022). For the extraction of anthocyanins, freeze-dried samples of plant leaves and stems from the H18 pepper were used. A 0.5 g sample was weighed and cut into small pieces, which a certain amount of quartz sand was added along with the pre-cooled extraction solution (1% HCl: 99% ethanol, v/v). The mixture was ground to a homogenized state, followed by the addition of 1% HCl-ethanol solution, and then the volume was adjusted to 25 mL. The solution was stored at 4°C for extraction in the shade for 20 min, with intermittent shaking. Three biological replicates were collected for each stage to minimize errors between samples. The extract was poured into a cuvette, and the absorbance was measured at 530 nm. The anthocyanin extract and the extraction solution (as a blank control) were poured into a cuvette, and the absorbance was measured at a wavelength of 530 nm. The concentration of total pepper anthocyanins was determined from a linear calibration curve prepared using the total anthocyanins from blueberry extract

(Yuan Ye Bio-Technology Co., Ltd., Shanghai, China).

2.3. Transcriptomic sequencing and analyzing

Three biological replicates of samples from each leaf development stage (S1, S2, S3, and S4) were collected to minimize errors between samples. RNA extraction, reverse transcription, and cDNA library construction were performed by a sequencing company (Personalbio, Nanjing, China). These libraries were subjected to paired-end (PE) sequencing using Next-Generation Sequencing (NGS) based on the Illumina sequencing platform. After filtering raw data, checking the sequencing error rate and checking the GC content distribution, clean reads were obtained by subsequent analysis. The unigene expression was quantified as TPM with the software package salmon (Alvarez *et al.* 2019). The raw data have been uploaded to the SRA database of NCBI (PRJNA1163342). The GO (http://www.geneontology.org/) functional database and KEGG (https://www.genome.jp/kegg/) pathway database were used to perform enrichment analysis on the differential gene set. Based on the results of KEGG enrichment analysis of DEGs, the top 20 pathways with the smallest *P*-value, i.e., the most significant enrichment, were selected for display (Kanehisa and Goto 2000; Burge *et al.* 2012).

2.4. Phylogenetic tree and expression analysis of *CaDFR*s

DFR belongs to the NADPH-dependent epimerase/dehydratase family (Ruan *et al.* 2022). Therefore, we performed a genome-wide search for the NADPH-dependent epimerase/dehydratase family in chili peppers by using the Simple HMM Search function in TBtools-II software (Chen *et al.* 2023). The specific steps are as follows: on the Simple HMM Search page of the TBtools software, input the protein sequences from the pepper genome, the profile hidden Markov models, and the Pfam number (PF01370) for the NADPH-dependent epimerase/dehydratase family to perform the search. Sequence alignment of proteins was performed by using the MUSCLE method in MEGA 7.0 software, and the phylogenetic tree was constructed with MEGA 7.0 software using the neighbor-joining (NJ) (bootstrap=1,000) (Kumar *et al.* 2016). Finally, TBtools software (Chen *et al.* 2020) was used to normalize the TPM data by using the $\log_2$(TPM) formula and Row Scale for processing and plotting the heatmap showing the expression of the identified genes.

2.5. Targeted anthocyanins metabolomic sequencing and analysis

The H18 pepper leaf samples were collected and ground into a powder (30 Hz, 1 min, with liquid nitrogen) using a ball mill, then extracted with 0.5 mL of hexane/acetone/ethanol mixture (1:1:1, v/v) containing 0.01% BHT (g mL^{-1}). The samples were vortexed for 20 min at room temperature, followed by centrifuged for 5 min at 4°C at 12,000 r min^{-1}. The supernatant was extracted, and the extraction process was repeated. The supernatant was extracted, and the extraction process was repeated once more. The supernatants were combined, concentrated, and redissolved in 100 μL of dichloromethane. The solution was passed through a 0.22 μm filter membrane and stored in a brown injection bottle for LC-MS/MS analysis. The data acquisition instrumentation system consisted of Ultra Performance Liquid Chromatography (UPLC) (ExionLC™ AD, https://sciex.com.cn/) and Tandem Mass Spectrometry (MS/MS) (QTRAP® 6500+, https://sciex.com.cn/). A MWDB (Metware Database) was constructed using standards to qualitatively analyze the data detected by mass spectrometry. Data quantification was accomplished by using the Multiple Reaction Monitoring (MRM) mode of triple quadrupole mass spectrometry, and then the precursor ions were induced to ionize by collision chambers. The precursor ions were induced to ionize by the collision chamber and broken to form multiple fragment ions, which were then filtered through a triple four-stage rod to select the required characteristic fragment ions, eliminating the interference of non-target ions. After obtaining the mass spectrometry data of different samples, the chromatographic peaks of all the targets were integrated and analyzed quantitatively by the MWDB (Metware Database) calibration curve.

2.6. Transient transformation of H18 pepper

The full-length CDS of *DFR1* was cloned from first-strand cDNA with 2× *TransStart® FastPfu* PCR SuperMix (+dye) (TransGen Biotech, Beijing, China). A specific *DFR1* fragment (216–546 bp) and *PDS* (819–1,179) was cloned into a pTRV2-C2b vector (Appendix A) (Zhou *et al.* 2021). The pTRV1 and the pTRV2-C2b constructs carrying the plasmid were transferred into *Agrobacterium* GV3101. H18 pepper plants with buds and only two cotyledons were used for transient transformation of VIGS. *Agrobacterium tumefaciens* containing pTRV1, pTRV2-C2b-*PDS*, and pTRV2-C2b-*DFR1* were injected into the cotyledons of the H18 pepper plants to be transformed, and the culture was resumed as normal after 48 h of dark incubation.

2.7. RNA extraction and cDNA synthesis

A total of three biological replicates of leaf samples from four different developmental stages and plants after VIGS transient transformation were harvested and flash frozen in liquid nitrogen until further processing for RNA extraction. Each biological replicate consisted of pooled tissue from the leaves of pepper. Samples were hand-ground in liquid nitrogen using a mortar and pestle before mRNA extraction. Total RNA was extracted using the TIANGEN RNAprep Pure Kit (Tiangen, Beijing, China) following the manufacturer's instructions. Reverse transcription was performed using a HiScript III 1st Strand cDNA Synthesis Kit (+gDNA wiper) (Vazyme Biotech, Najing, China). Includes three reaction steps: RNA template denaturation, genomic DNA removal and first-strand cDNA synthesis reaction.

2.8. RT-qPCR analysis

All RT-qPCR primers were designed using Beacon Designer 7 software (Appendix A). RT-qPCR was performed with a CFX96 TouchTM Real-Time PCR Detection System (BIO-RAD, USA), with three biological replicates for each sample. The relative gene expression levels were calculated using

the $2^{-\Delta\Delta CT}$ method (Livak and Schmittgen 2001). *CaACT* (Genebank: AY572427.1) was used as a reference gene for H18 pepper qPCR (Wan *et al.* 2011).

2.9. Construction of the *CaDFR*s expression vector and induced purification of recombinant protein

The full-length coding sequence of *CaDFR*s was cloned and then expressed in the pGEX4T-1 vector (GE Healthcare, Chicago, IL, USA). Recombinant pGEX4T-1-*CaDFRs* was transformed into *E. coli* BL21 (DE3)-competent cells. The culture was expanded to an OD value of approximately 0.6, and isopropyl-β-D-thioacetamide IPTG was added to a final concentration of 1 mmol L^{-1} to induce the fusion expression of the target protein and GST binding protein. Finally, the cells were cultured with shaking at 16°C for 24 h, and the cells were collected by centrifugation at 4°C. Affinity chromatography resin with GST tag GST·Bind™ resin (TransGen Biotech, Beijing, China) was used to purify the protein, and elution buffer (pH 8.0) was used for GST-Sefinose™ resin (containing reducing glutathione reagent at a concentration of 1.538 g L^{-1}) elution.

2.10. Enzyme activity assay

The enzymatic reaction consisted of 0.1 mol L^{-1} pH 7.0 potassium phosphate buffer, 2 mmol L^{-1} NADPH, 1 mmol L^{-1} DHQ, DHM, and DHK, and 0.05 mg total soluble proteins. The reaction mixtures were incubated at 30°C for 12 h, and the total volume was 200 μL. Because leucoanthocyanidin is unstable in solution and difficult to detect directly using HPLC, a 3× volume of butanol-HCl reagent (95:5, v/v) was added, and the reaction was split at 95°C for 1 h to form anthocyanidin, then centrifuged at 4,000×g for 15 min.

2.11. Data collection and statistical analysis

Data presented are means±SE of at least three independent experiments. The experimental data were analyzed by one-way ANOVA (P<0.05). Statistical analyses were performed using GraphPad Prism 8.0 software.

3. Results

3.1. Phenotypic characterization and determination of anthocyanin content in H18 pepper leaves

The leaves of the H18 variety are completely purple and darker in color during the cotyledon stage (5 days after germination, S1). In the early development stage of the plant, the true leaves (12 days after germination, S2) are also completely purple, although lighter than those at the cotyledon stage. As the plant continues to grow, a new stage emerges (20 days after germination, S3), where the leaves exhibit both purple and green colors. In the true leaf green stage (30 days after germination, S4), the leaves are completely green (Fig. 1-A). We measured the anthocyanins in the leaves during these four stages and observed a gradual decline, which was generally consistent with the changes in leaf color (Fig. 1-B).

3.2. Targeted metabolomic analysis of anthocyanins in H18 pepper leaves

We conducted targeted metabolomic assays of anthocyanins

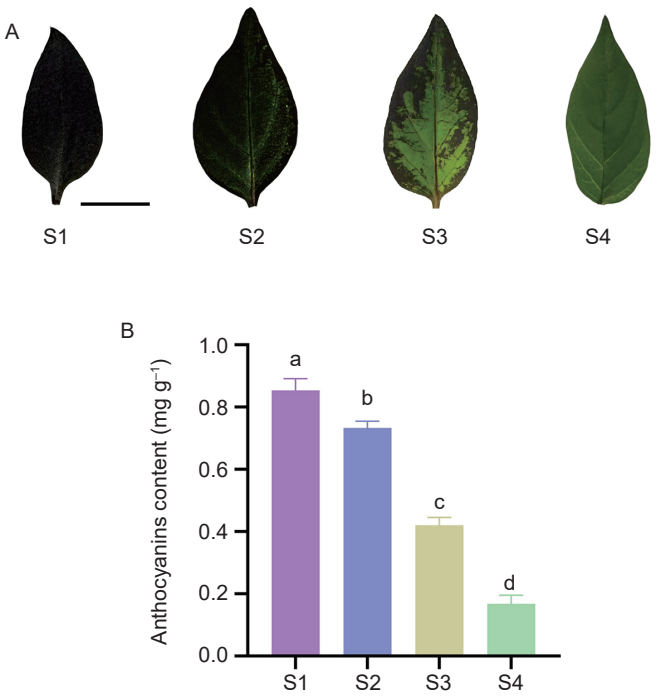


Fig. 1 Phenotypic observation and anthocyanin content determination of H18 pepper leaves at four developmental stages (S1–S4). A, phenotypes of of leaves at S1, S2, S3, and S4. Scale bar=1 cm. B, anthocyanin contents in leaves at S1, S2, S3, and S4. Data are presented as mean±SD from three replicates (n=3). Different letters indicate significant differences at P<0.05 according to one-way or two-way ANOVA (Duncan's multiple range test).

in leaves at different developmental stages. A total of 51 types of anthocyanins modified by glycosylation or acylation were detected from cyanidin, peonidin, delphinidin, malvidin, petunidin and pelargonidin (Fig. 2; Appendix B). Additionally, two types of flavonoids, quercetin-3-*O*-glucoside and naringenin, were identified. Our data analysis revealed that cyanidin derivatives are primarily found in the cotyledons of H18 chili pepper plants, with lower prevalences in the true leaves. In contrast, pelargonidin derivatives are predominantly present in the true leaves of H18 chili pepper plants. A series of anthocyanins, including delphinidin, malvidin, and petunidin, which are produced from DHM through the catalyze of DFR, ANS, and UGT, constitute the main components of anthocyanins in H18 pepper leaves (Fig. 2-A; Appendix B). Furthermore, after normalizing the data, we find that the trend of their content aligns with our measurements of total anthocyanin levels, showing a gradual decline (Fig. 2-A). The data that has not been normalized revealed that delphinidin-3-*O*-rutinoside, delphinidin-3-(6′′-*O*-coumaroyl) rutinoside-5-*O*-glucoside, delphinidin-3-*O*-glucoside and delphinidin-3-*O*-galactoside significantly higher than other types of anthocyanins and the highest content among them was delphinidin-3-*O*-rutinoside (Fig. 2-B). Therefore, we conclude that delphinidin, malvidin, and petunidin are the primary contributors to the purple coloration of H18 pepper leaves, with delphindin playing the most significant role.

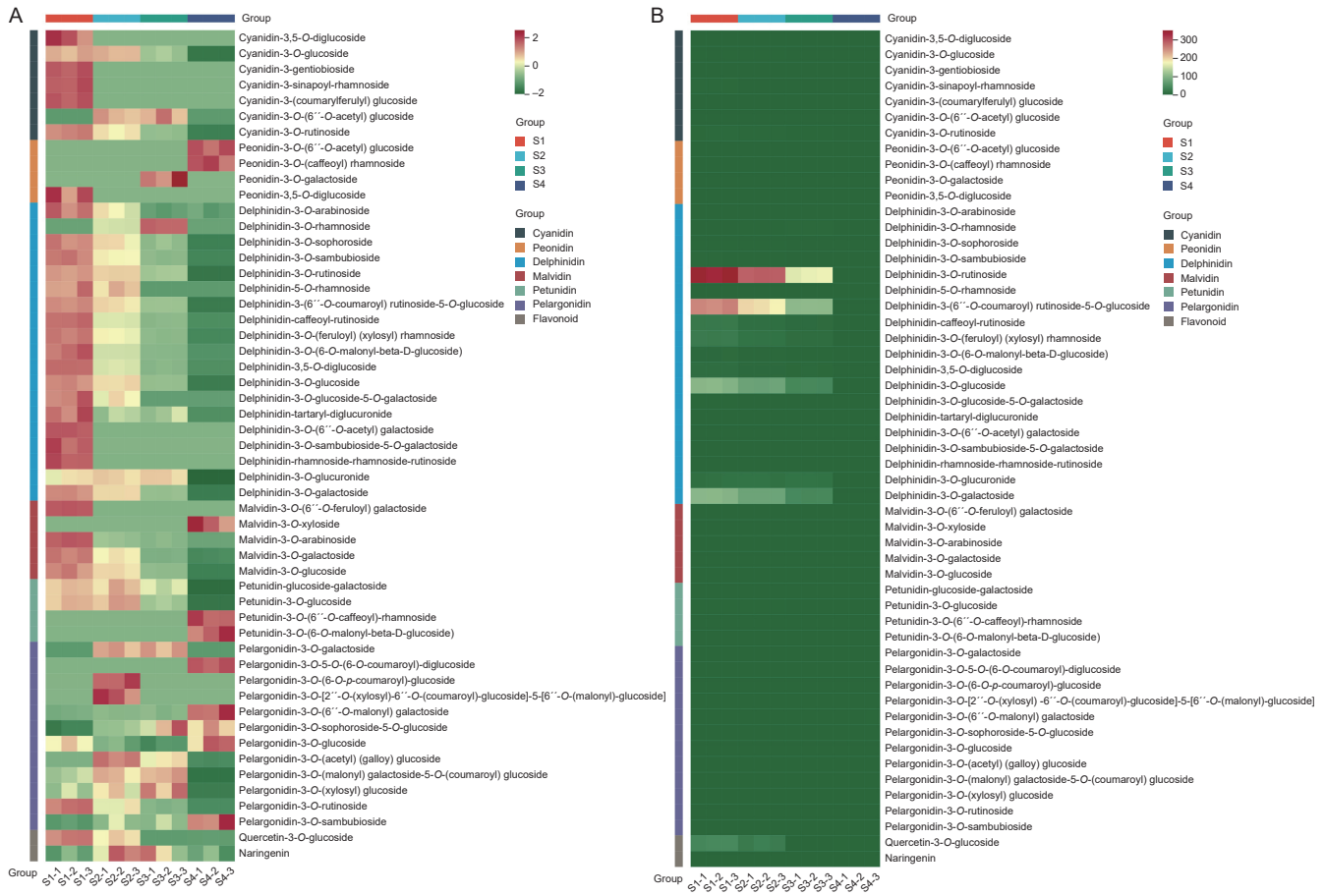


Fig. 2 Heatmap analysis of targeted anthocyanin data. A, normalized metabolomic data for targeted anthocyanins. B, targeted anthocyanin metabolomic data without normalization.

3.3. Analysis of transcriptomic of H18 pepper leaves with different development stages

We conducted GO and KEGG analyses of differentially expressed genes (DEGs) to elucidate the enriched functions and pathways of these genes. The GO analysis results indicated significant enrichment of DEGs in biological processes and molecular functions, and cellular components across the comparisons S1 *vs*. S4, S2 *vs*. S4, and S3 *vs*. S4. Furthermore, from S1 to S3, compared to S4, the enrichment of DEGs in biological process and molecular function gradually decreased, while the enrichment in cellular component increased (Fig. 3-A–C). The KEGG analysis results revealed significant enrichment of genes associated with flavonoid biosynthesis pathway in S1 *vs*. S4, S2 *vs*. S4, and S3 *vs*. S4 comparisons. Flavonoid biosynthesis is closely linked to the synthesis of anthocyanins and flavonoids. Additionally, as leaf developmental stages (S1–S3), compared to S4, the number of DEGs enriched in the flavonoid biosynthesis pathway gradually decreased, while the false discovery rate (FDR) increased (Fig. 3-D and E).

3.4. Identification, phylogenetic tree, and expression analysis of the *DFR* gene family

In the previous section, we concluded through transcriptomic analysis that the variation in H18 leaves color is strongly correlated with the flavonoid biosynthesis pathway. *DFR*, a key enzyme in determining the type of anthocyanins, is central to this study, which focuses on investigating the functions of the *DFR* gene family. As the *DFR* gene family belongs to the NADPH-dependent epimerase/dehydratase family, we performed a whole-genome identification of NADPH-dependent epimerase/dehydratase genes in chili peppers. A total of 170 such genes were identified (Fig. 4-A; Appendix C). Subsequently, we constructed a phylogenetic tree by analyzing the pepper NADPH-dependent epimerase/dehydratase genes alongside the functional *DFR* genes from eggplant (Wang *et al.* 2022) and tea (Ruan *et al.* 2022). Transcriptomic expression analysis was conducted on these genes (Appendix C; Fig. 4-A). We found that several functional genes clustered with the NADPH-dependent epimerase/dehydratase genes in chili peppers, leading us to believe that all genes in this branch are *DFR* genes (Fig. 4-A). Moreover, we identified the genes *Capana02g002763* (*CaDFR1*), *Capana00g003773* (*CaDFR2*) and *Capana03g000475* (*CaDFR3*) as being consistent with the trend of anthocyanin content in H18 leaves (S1–S4), which showed a gradual decrease. These three genes were therefore considered as candidates *DFR* genes. We applied the same method to analyze

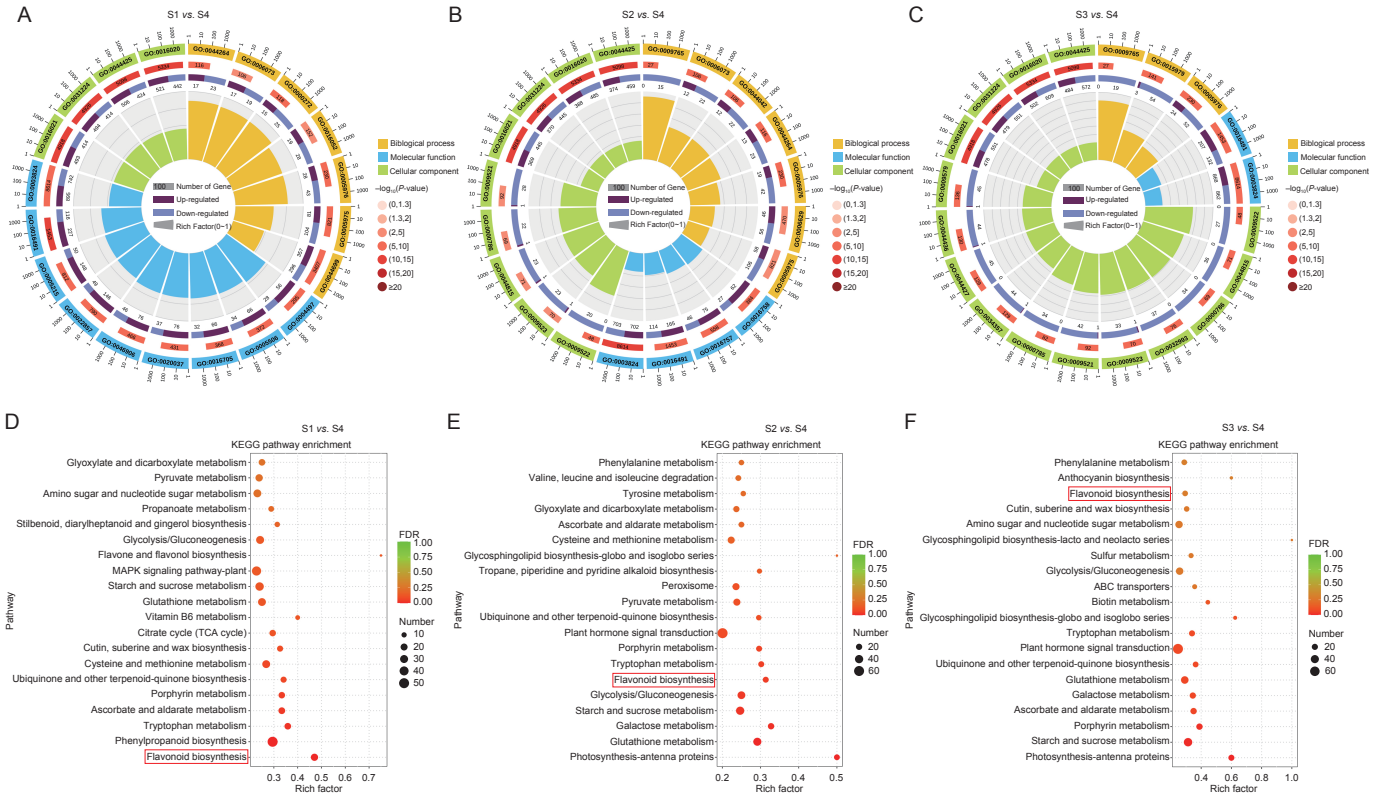


Fig. 3 Transcriptomics analysis of H18 pepper leaves at four different developmental stages (S1–S4). A–C, GO enrichment analysis of differentially expressed genes (DEGs) from S1 *vs*. S4, S2 *vs*. S4, and S3 *vs*. S4 comparisons, respectively. D–F, KEGG pathway analysis of DEGs from the same comparisons.

members of other gene families involved in the H18 pepper anthocyanin biosynthetic pathway, such as *CaCHS*, *CaCHI*, and *CaF3H*, identifying their corresponding candidate functional genes (Fig. 4-B).

3.5. Substrate catalytic analysis of recombinant proteins of CaDFRs

*CaDFR*s were cloned into the pGEX-4T-1 vector, and the recombinant proteins GST-CaDFR1, GST-CaDFR2, GST-CaDFR3 were induced and purified. SDS-PAGE electrophoretogram showing the target bands in the supernatant of *E. coli* carrying the recombinant plasmid after IPTG induction, in the precipitate, and after purification of the supernatant (Appendix D). In the process substrate catalysis for CaDFRs, leucoanthocyanidins produced by DHQ, DHK, and DHM catalyzed by DFR enzyme are extremely unstable and difficult to detect directly by HPLC. Therefore, we used the Bate-Smith method (Bate-Smith 1973), in which the leucoanthocyanidins produce red anthocyanidins when heated under acidic conditions, for detection. The results of the catalytic experiments indicate that when DHQ, DHK, and DHM are used as substrates, CaDFR2 and CaDFR3 do not produce any red anthocyanins. However, CaDFR1 was able to effectively catalyze the reaction of DHQ, DHK, and DHM, resulting in the cleavage and production of red anthocyanins (Fig. 5). This suggests that CaDFR2, CaDFR3 lack catalytic activity towards DHQ, DHK, and DHM, whereas CaDFR1 exhibits strong catalytic activity towards these three substrates.

3.6. Amino acid sequence analysis between DFRs

Previous studies have shown that the DFR in *Arabidopsis* and tea (*Camellia sinensis*) plants can catalyze three substrates: DHQ, DHM, and DHK (Chen *et al.* 2020; Ruan *et al.* 2022). In contrast, the PhDFR in petunia (*Petunia hybrida*) can catalyze only two substrates, DHQ and DHM, and is unable to catalyze DHK (Forkmann and Ruhnau 1987; Johnson *et al.* 2001). The DFR in cranberry (*Vaccinium macrocarpon*) is limited to catalyzing only the substrate DHQ (Polashock *et al.* 2002). Most species have D (aspartic) or N (asparagine) at position 134, and E (glutamic) at position 145. In petunia, the amino acid at position 145 is Q (glutamine acid), while in cranberry, the VmDFR1-1 contains V (valine) at position 134 (Johnson *et al.* 2001; Polashock *et al.* 2002). These characteristics are likely the reasons why they cannot catalyze all three substrates (DHQ, DHM, and DHK). Amino acid sequence alignment revealed that the catalytically functional CaDFR1 shares strong similarity with AtDFR, CsDFRa, PhDFR, and VmDFR1-1, particularly in the conserved regions of the amino acid sequences including NADPH binding site and the substrate binding site (Fig. 6). Specifically, at position 134, CaDFR1 contains D (aspartic), and at position 145, it contains E (glutamic). Furthermore, CaDFR2 and CaDFR3 also show a strong conservation of amino acid sequences in the NADPH binding site, but substrate binding site is different from the catalytically functional *DFR* genes. Position 134 of the CaDFR2 amino acid sequence is V (valine), which is

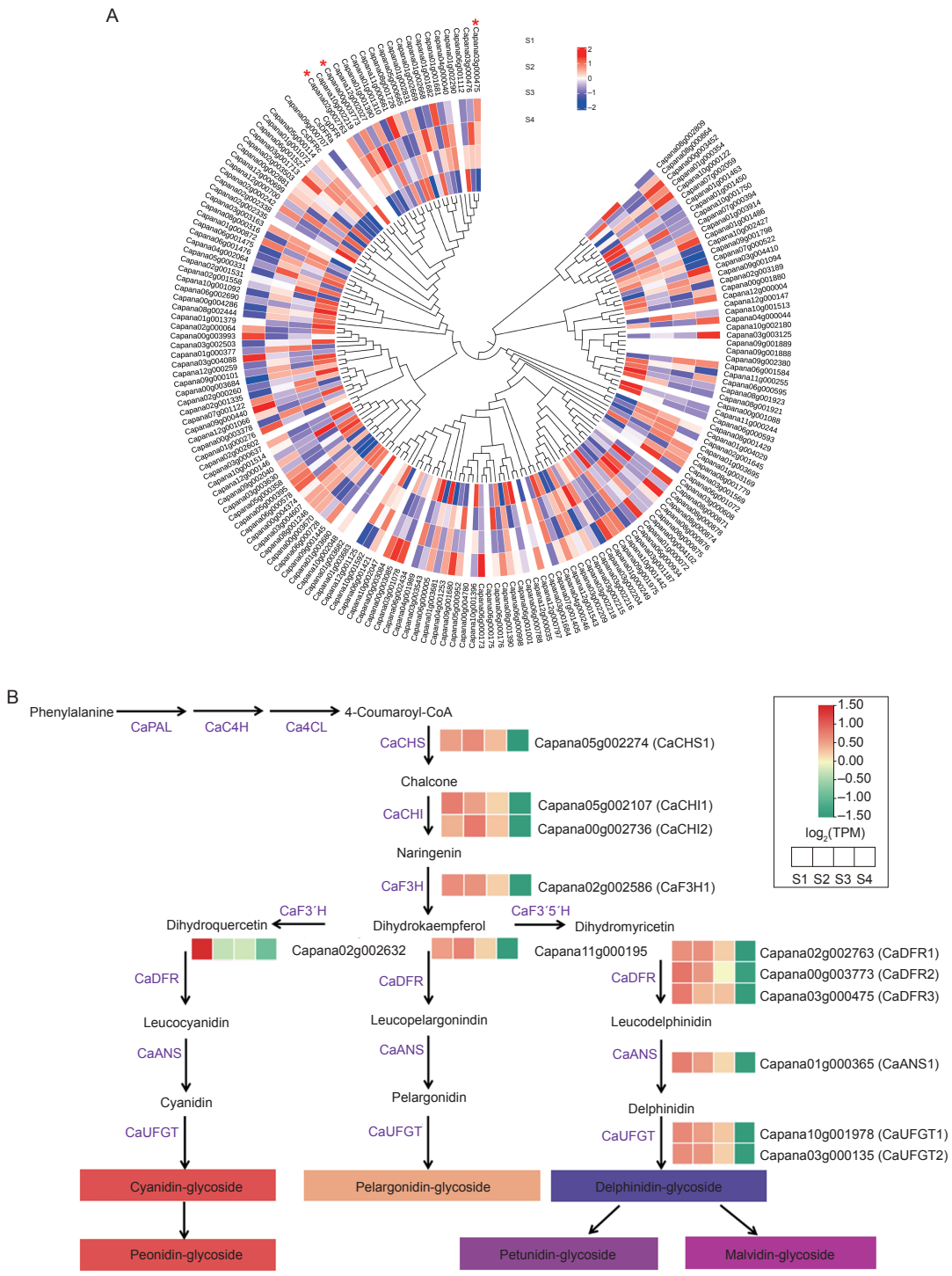


Fig. 4 Identification of dihydroflavonol 4-reductase (*DFR*) candidate genes and transcriptomics analysis of anthocyanins metabolic pathway. A, phylogenetic tree and expression analysis of the *DFR* gene family. B, analysis of gene expression levels in anthocyanin metabolism pathways.

identical to VmDFR1-1 and CaDFR3 is Y (tyrosine). Position 145 of the amino acid sequence of both genes is E (glutamic acid) (Fig. 6). However, no catalytic activity was detected for these two genes. Therefore, the inactivity of CaDFR2 suggests that the activity of DFR is not simply determined by the amino acids at positions 134 and 145 of the substrate binding region (Fig. 6). Instead, alterations in each amino acid within this binding site may influence DFR activity, and the amino acid sites affecting DFR function require further investigation.

3.7. Analysis of VIGS-mediated *CaDFR1* gene silencing in H18 pepper leaves

Based on the previous section, we have determined that

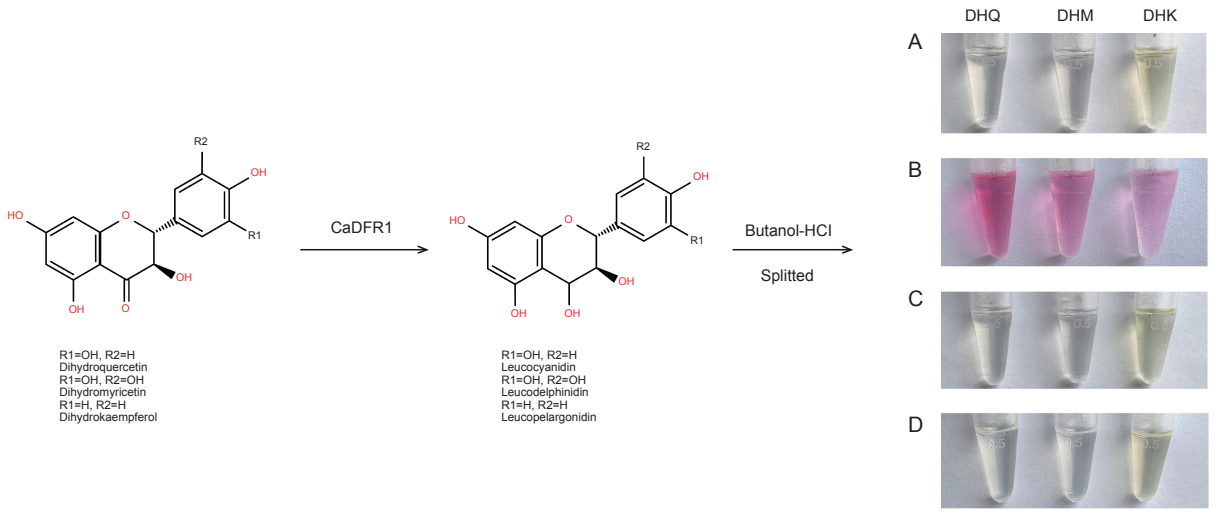


Fig. 5 Analyses of catalytic reaction products with CaDFR fusion proteins. A, GST protein. B, CaDFR1 protein. C, CaDFR2 protein. D, CaDFR3 protein. DHQ, dihydroquercetin; DHM, dihydromyricetin; DHK, dihydrokaempferol.

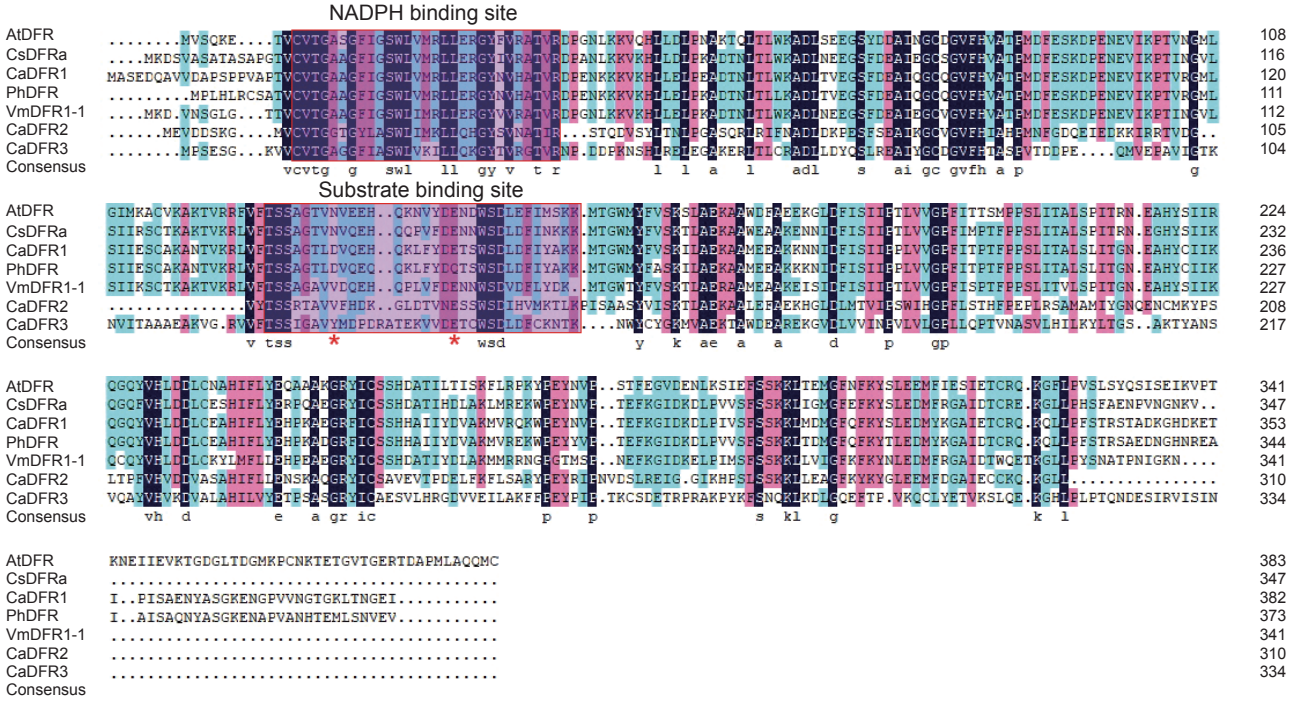


Fig. 6 Multiple sequence alignment of dihydroflavonol 4-reductases (DFRs) from various plant species. The NADPH-binding region and substrate-binding site are boxed in red. AtDFR (AED94866), CsDFRa (KY615690), PhDFR (X15537.1), and VmDFR1-1 (AF483835).

CaDFR1 can catalyze three substrates (DHQ, DHM and DHK), playing a crucial role in anthocyanins synthesis. Therefore, we aim to utilize VIGS-mediated gene silencing technology to confirm the function of *CaDFR1*. In this study, we first observed plant traits by silencing the *CaPDS* gene. The results showed that after silencing *CaPDS* in the H18 pepper plant led to a reduction in chlorophyll content in the newly grown stems and leaves (Fig. 7-A). After silencing *CaDFR1*, RT-qPCR analysis revealed a significant decrease in the expression level of *CaDFR1*, confirming the success of our silencing experiment (Fig. 7-B and C). Compared to the control group, the newly developed stems and leaves of the silenced plants predominantly exhibit green traits, with a significant reduction of purple on the leaves and stems (Fig. 7-A). This observation is consistent with chlorophyll loss in H18 plants following *CaPDS* silencing. Subsequently, we measured the anthocyanin content in the leaves and stems of both the silenced and control plants. The results revealed a significant reduction of anthocyanin in the H18 leaves and stems following *CaDFR1* silencing compared to the control group (Fig. 7-D). This further confirms the crucial role of *CaDFR1* in anthocyanin biosynthesis in H18 plants.

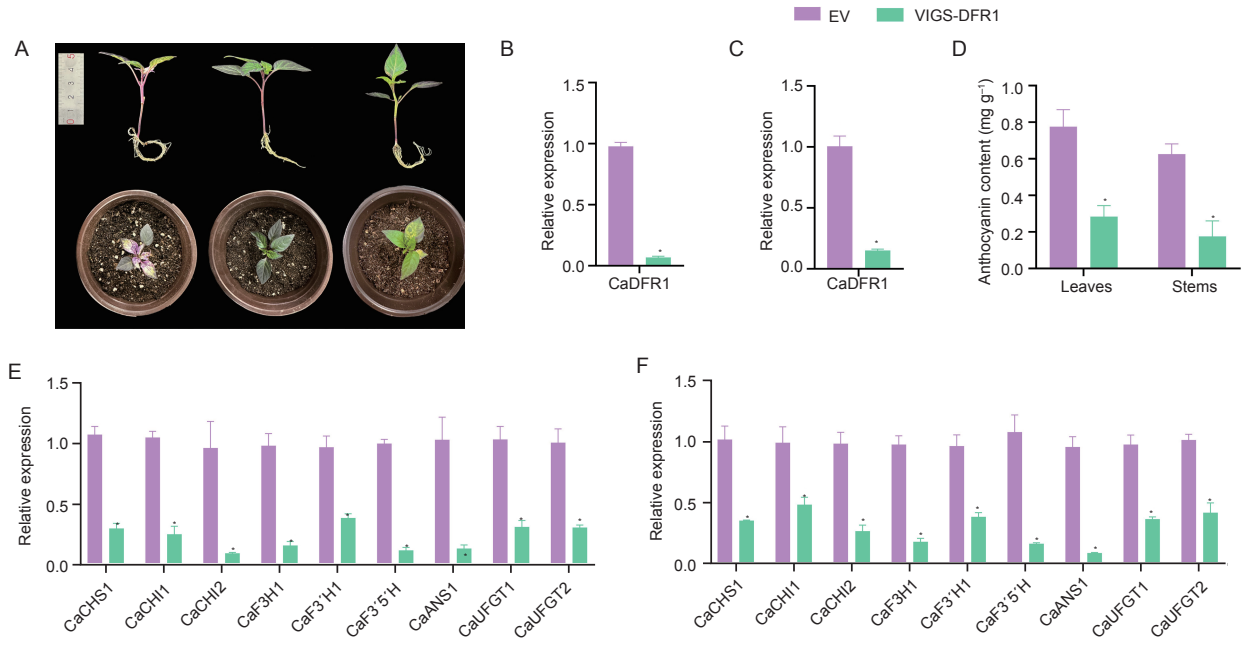


Fig. 7 Analysis after VIGS silencing of *CaDFR1* and *CaPDS* in H18 pepper leaves. A, phenotypic observations after VIGS silencing of H18 pepper plants. B, RT-qPCR analysis of *CaDFR1* in pepper leaves. C, RT-qPCR analysis of *CaDFR1* in pepper stems. D, analysis of anthocyanin content in H18 pepper plants after VIGS silencing of *CaDFR1*. E, RT-qPCR analysis of candidate genes on the anthocyanin metabolic pathway in pepper leaves. F, RT-qPCR analysis of candidate genes on the anthocyanin metabolic pathway in pepper stems. Data are presented as mean±SD from three replicates (n=3). *, P<0.05 according to one-way or two-way ANOVA (Duncan's multiple range test).

Subsequently, we performed an expression analysis of other candidate functional genes in the anthocyanin metabolic pathway using RT-qPCR. The results showed that the expression levels of these genes in the stems also decreased following *CaDFR1* silencing (Fig. 7-E and F). This provides further evidence of the pivotal role of *CaDFR1* in regulating anthocyanin biosynthesis in H18 chili peppers.

4. Discussion

Anthocyanins are a major subclass of flavonoids that play various important roles in plants, including UV radiation resistance, involvement in hormone regulation, and response to biotic and abiotic stress (Zhang *et al.* 2016; Sun *et al.* 2021; Zhu *et al.* 2024). Additionally, anthocyanins are beneficial to human health (Mattioli *et al.* 2020; Mujanović *et al.* 2024). In the Solanaceae family, the most common anthocyanins are found in eggplant fruits, with studies showing that all wild eggplant varieties exhibit extensive anthocyanin accumulation patterns in their pericarp and petals (Wang *et al.* 2022). Anthocyanin-rich purple tomato fruit varieties have been developed through conventional breeding, transgenics, and gene editing in tomato research on anthocyanins (Butelli *et al.* 2008; Sun *et al.* 2020). Research has also explored the use of purple anthocyanin markers in male-sterile tomato varieties to differentiate between fertile and sterile seeds, thereby enhancing the efficiency and convenience of breeding of male-sterile tomatoes (Du *et al.* 2020). In this study, we analyzed the leaves of purple pepper varieties to investigate the key genes responsible for the purple coloration, providing valuable insights for future breeding of purple peppers.

The orchid genus *Cymbidium* includes species that produce flowers in white, yellow, green, pink, purple, and red flowers but notably lacks orange-colored flowers due to only the presence of cyanidin and peonidin-based anthocyanins as identified in a survey of two species and seven cultivars (Nakatsuka *et al.* 2019). Similarly, roses (*Rosa rugosa*) and gerberas never produce delphinidin and never carry blue flowers (Helariutta *et al.* 1993; Katsumoto *et al.* 2007). In purple-fleshed sweet potato (PFSP), a total of 42 anthocyanin monomers were identified, with cyanidin and peonidin being the major aglycones constituting PFSP anthocyanins (Huang *et al.* 2021). In this study, we observed a gradual decrease in anthocyanin levels in H18 pepper leaves at different developmental stages. Targeted analysis of anthocyanin metabolites revealed that delphinidin, malvidin, and petunidin are the major components, and their content trends are consistent with the overall trend of anthocyanin changes, particularly delphinidin. This study demonstrated that the color of H18 chili pepper leaves is primarily influenced by the anthocyanin catalytic pathway using DHM as a substrate.

A wealth of research has been conducted on the color of plant fruits and leaves, with most studies focusing on transcriptomics, metabolomics, and gene functional validation analyses. The conclusions of these studies are generally consistent, indicating that changes in plant pigments are often related to variations in anthocyanins or carotenoids. Transcriptomic analyses reveal that enrichment analysis of differentially expressed genes often identifies gene clusters involved in flavonoid or carotenoid metabolic pathways (Shi *et al.* 2020; He *et al.* 2023; Rodríguez-Lorenzo *et al.* 2023; Xu *et al.* 2024). Our study on the leaves of H18 pepper exhibits certain similarities to previous research,

particularly that the leaf decoloration is linked to changes in anthocyanins. Furthermore, transcriptomic analysis indicates that a significant number of differentially expressed genes are enriched in flavonoid metabolic pathways, with alterations in key genes involved in anthocyanin metabolism, such as the *DFR* gene.

The amino acid sequences of DFR across different species exhibit high homology in numerous regions, with the NADP binding site of the protein being particularly conserved region among various species (Aiguo *et al.* 2022). However, different species of DFR exhibit varying substrate preferences. For instance, the AtDFR in *Arabidopsis*, CsDFRa and CsDFRc in tea, and MaDFR in Grape hacinth (*Muscari* spp.) are all capable of catalyzing the three substrates DHK, DHQ, and DHM (Liu *et al.* 2019; Chen *et al.* 2020; Ruan *et al.* 2022). The GDFR1-1, GDFR1-2, and GDFR1-3 in gerbera are only active towards the two substrates DHQ and DHK, while the DFR in *Cymbidium* (*Cymbidium* hybrids) and petunia can only catalyze DHQ and DHM. In contrast, the DFR in cranberry (*Vaccinium macrocarpon*) is capable of catalyzing only the substrate DHQ (Forkmann and Ruhnau 1987; Johnson *et al*. 1999; Polashock *et al*. 2002; Bashandy *et al*. 2015; Nakatsuka *et al*. 2019). Research indicates that the substrate selectivity of DFR is closely associated with its substrate binding site. The amino acids at positions 134 and 145 in the substrate binding site directly influence the substrate specificity of the enzyme. Most species have D (aspartic) or N (asparagine) at position 134, whereas cranberry has V (valine) at this position, which restricts its DFR enzyme activity to only the substrate DHQ (Johnson *et al*. 1999, 2001; Polashock *et al*. 2002). Replacing the N (asparagine) at position 134 of the gerbera DFR with the nonpolar L (leucine) and introducing it into petunia revealed that the N134L mutant DFR of gerbera preferentially converts DHK rather than DHQ and DHM. Furthermore, replacing the E (glutamic) at position 145 of gerbera DFR with L (leucine) results in the E145L mutant DFR being unable to reduce DHK (Johnson *et al.* 2001). Therefore, the amino acids at positions 134 and 145 in gerbera DFR (the substrate binding site) directly influence substrate specificity. In *Medicago truncatula*, MtDFR2 has an aspartic acid (D) at the corresponding position 134 and can convert DHK according to *in vitro* enzyme analysis, whereas MDFR1 has N (asparagine) at this position, and the efficiency of DHK, as shown by conversion (catalytic activity of MtDFR1 for DHK is about 2.5 times that of MtDFR2). This further confirms that the amino acid type at position 145 directly determines both the ability of DFR to convert DHK and the efficiency of the conversion (Xie *et al.* 2004). In our sequence alignment, we found that the amino acid sequence of CaDFR1 in chili pepper has D (aspartic) at site 134 and E (glutamic) at site 145. This characteristic indicates that the reason why CaDFR1 is capable of catalyzing three different substrates.

The different anthocyanins present in plants lead to a wide range of colors. Delphinidin and its methylated derivatives, petunidins, and malvidins are sources of dark bluish and purple colors, while cyanidins and pelargonidins are the main pigments in bright red colored fruits (Jaakola *et al.* 2002; Jaakola 2013). In *Arabidopsis*, the DFR-deficient mutant *tt3* exhibits a complete lack of PA accumulation and hyaline testa, whereas DFR-deficient gerbera has a phenotype with white petals (Kubasek *et al.* 1992; Bashandy *et al.* 2015). The study found that knocking out the *DFR1*/*DFR2* genes in tobacco (*Nicotiana tabacum*) using CRISPR/Cas9 resulted in a significant change in flower color: *DFR* gene knockout (*DFR*-KO) tobacco flowers were white, while the wild type (CK) flowers were red (Jiang *et al.* 2023). In this study, we employed VIGS technology to silence *CaDFR1*. The results showed that the newly grown stems and leaves of silenced *CaDFR1* plants exhibited a significant reduction in anthocyanin levels compared to the control group, further validating the important role of *CaDFR1* in anthocyanin synthesis in H18 pepper.

In osteospermum (*Osteospermum hybrida*), DFR cannot catalyze DHK, resulting in blue-colored flowers. By employing RNA interference technology to inhibit the expression of the *F3´5´H* gene in osteospermum while overexpressing the *DFR* gene from Gerbera, a large accumulation of Pelargonidin occurred, ultimately resulting in red flowers (Seitz *et al.* 2007). Roses (*Rosa hybrida*) lack purple to blue flower varieties due to the absence of anthocyanins based on delphinidin. In the rose purple-flowered cultivar Lavanda, overexpression of the *F3´5´H* gene from viola (*Viola* spp.) and the *DFR* gene from *Iris hollandica* (which can effectively catalyze DHM) was performed, along with RNAi-mediated downregulation of its own *DFR* gene. This led to the substantial accumulation of delphinidin, ultimately giving the flowers a blue color (Katsumoto *et al*. 2007; Tanaka *et al*. 2009). Genetic modification of *DFR* and other genes involved in anthocyanin pathways to alter the color of plant organs presents broad application prospects. Subsequent research intends to conduct experiments on chili pepper plants to produce high-quality, multi-colored chili pepper varieties.

5. Conclusion

In this study, based on the characteristics of the gradually disappearing pigment in the leaves of H18 chili peppers during development, we selected leaves from different developmental stages (S1–S4) for physiological and biochemical tests, targeted anthocyanin metabolite analysis, and transcriptomic sequencing. The results showed that as the plants developed, the content of anthocyanins in the leaves decreased, and delphinidin, malvidin, and petunidin derivatives showed a consistent trend with the changes in anthocyanin contents in H18 pepper leaves. Among them, delphinidin-3-*O*-rutinoside, delphinidin-3-(6´´-*O*-coumaroyl) rutinoside-5-*O*-glucoside, delphinidin-3-*O*-glucoside, and delphinidin-3-*O*-galactoside occupy a major part of the anthocyanin content. Analysis of the transcriptomic sequencing data also indicates that most of the DEGs are concentrated in the flavonoid metabolism pathway. Combined with expression levels and phylogenetic tree analysis, we screened *Capana02g002763* (*CaDFR1*), *Capana00g003773* (*CaDFR2*), and *Capana03g000475* (*CaDFR3*), — three *DFR* candidate genes — and other gene family candidates in the anthocyanin metabolism pathway. Enzyme activity analysis revealed that only CaDFR1 exhibits

substrate catalytic activity, capable of catalyzing the DHQ, DHM, and DHK substrates. VIGS silencing of the *CaDFR1* gene showed that the silenced H18 pepper plants had a significant decrease in anthocyanin content in new stems and leaves. In summary, through a series of studies, we have elucidated the key anthocyanin metabolism mechanism in the leaves of H18 chili pepper and validated the function of the key gene *CaDFR1* in the anthocyanin metabolism pathway, providing a theoretical basis for the selection of chili pepper varieties related to anthocyanins through molecular methods.

Acknowledgements

This work was supported by the Postdoctoral Research Program Support of Anhui Province, China (2024C863), the China Agriculture Research System of MOF and MARA (CARS-23-G40, CARS-23-G49), and the Youth Development Fund from Anhui Academy of Agricultural Science, China (QNYC-202121). Thanks to Prof. Feng Li, College of Horticulture and Forestry, Central China Agricultural University, for providing the TRV2-C2b vector.

Declaration of competing interest

The authors declare that they have no conflict of interest.

Declaration of generative AI and AI-assisted technologies in the writing process

During the preparation of this manuscript, the authors used ChatGPT 4.0 to assist in improving the clarity and readability of the language. All content generated was carefully reviewed and revised by the authors as necessary, and the authors take full responsibility for the final content of the article.

Appendices associated with this paper are available at https://doi.org/10.1016/j.jia.2025.10.011

References

Aiguo Z, Ruiwen D, Cheng W, Cheng C, Dongmei W. 2022. Insights into the catalytic and regulatory mechanisms of dihydroflavonol 4-reductase, a key enzyme of anthocyanin synthesis in *Zanthoxylum bungeanum*. *Tree Physiology*, **43**, 169–184.

Araguirang G E, Richter A S. 2022. Activation of anthocyanin biosynthesis in high light — what is the initial signal? *New Phytologist*, **236**, 2037–2043.

Baenas N, Belović M, Ilic N, Moreno D A, García-Viguera C. 2019. Industrial use of pepper (*Capsicum annum* L.) derived products: Technological benefits and biological advantages. *Food Chemistry*, **274**, 872–885.

Bashandy H, Pietiäinen M, Carvalho E, Lim K J, Elomaa P, Martens S, Teeri T H. 2015. Anthocyanin biosynthesis in gerbera cultivar 'Estelle' and its acyanic sport 'Ivory'. *Planta*, **242**, 601–611.

Bate-Smith E C. 1973. Haemanalysis of tannins: The concept of relative astringency. *Phytochemistry*, **12**, 907–912.

Bharti A K, Khurana J P. 2003. Molecular characterization of *transparent testa* (*tt*) mutants of *Arabidopsis thaliana* (ecotype Estland) impaired in flavonoid biosynthetic pathway. *Plant Science*, **165**, 1321–1332.

Burge S, Kelly E, Lonsdale D, Mutowo-Muellenet P, McAnulla C, Mitchell A, Sangrador-Vegas A, Yong S Y, Mulder N, Hunter S. 2012. Manual GO annotation of predictive protein signatures: the InterPro approach to GO curation. *Database* (Oxford), **2012**, bar068.

Butelli E, Titta L, Giorgio M, Mock H P, Matros A, Peterek S, Schijlen E G, Hall R D, Bovy A G, Luo J, Martin C. 2008. Enrichment of tomato fruit with health-promoting anthocyanins by expression of select transcription factors. *Nature Biotechnology*, **26**, 1301–1308.

Cackett L, Luginbuehl L H, Schreier T B, Lopez-Juez E, Hibberd J M. 2022. Chloroplast development in green plant tissues: the interplay between light, hormone, and transcriptional regulation. *New Phytologist*, **233**, 2000–2016.

Cerqueira J V A, de Andrade M T, Rafael D D, Zhu F, Martins S V C, Nunes-Nesi A, Benedito V, Fernie A R, Zsögön A. 2023. Anthocyanins and reactive oxygen species: a team of rivals regulating plant development? *Plant Molecular Biology*, **112**, 213–223.

Chen C, Wu Y, Li J, Wang X, Zeng Z, Xu J, Liu Y, Feng J, Chen H, He Y, Xia R. 2023. TBtools-II: A "one for all, all for one" bioinformatics platform for biological big-data mining. *Molecular Plant*, **16**, 1733–1742.

Chen X, Liu W, Huang X, Fu H, Wang Q, Wang Y, Cao J. 2020. Arg-type dihydroflavonol 4-reductase genes from the fern *Dryopteris erythrosora* play important roles in the biosynthesis of anthocyanins. *PLoS ONE*, **15**, e0232090.

Davies K M, Landi M, van Klink J W, Schwinn K E, Brummell D A, Albert N W, Chagné D, Jibran R, Kulshrestha S, Zhou Y, Bowman J L. 2022. Evolution and function of red pigmentation in land plants. *Annals of Botany*, **130**, 613–636.

Du M, Zhou K, Liu Y, Deng L, Zhang X, Lin L, Zhou M, Zhao W, Wen C, Xing J, Li C B, Li C. 2020. A biotechnology-based male-sterility system for hybrid seed production in tomato. *Plant Journal*, **102**, 1090–1100.

Espley R V, Jaakola L. 2023. The role of environmental stress in fruit pigmentation. *Plant, Cell & Environment*, **46**, 3663–3679.

Fang K, Liu Y, Wang Z, Zhang X, Zou X, Liu F, Wang Z. 2025. Genome-wide analysis of the CaYABBY family in pepper and functional identification of *CaYABBY5* in the regulation of floral determinacy and fruit morphogenesis. *Journal of Integrative Agriculture*, **24**, 3024–3039.

Forkmann G, Ruhnau B J Z f N C. 1987. Distinct substrate specificity of dihydroflavonol 4-reductase from flowers of *Petunia hybrida*. *Zeitschrift fur Naturforschung* (C), **42**, 1146–1148.

He S, Ye Y, Yuan Y, Lv M, Wang M, Xu Q, Xu X, Chen X. 2023. Insights into flavonoid biosynthesis during cucumber fruit peel coloration based on metabolite profiling and transcriptome analyses. *Horticultural Plant Journal*, **9**, 763–776.

Helariutta Y, Elomaa P, Kotilainen M, Seppänen P, Teeri T H. 1993. Cloning of cDNA coding for dihydroflavonol-4-reductase (DFR) and characterization of *dfr* expression in the corollas of *Gerbera hybrida* var. Regina (Compositae). *Plant Molecular Biology*, **22**, 183–193.

Huang Y, Zhou S, Zhao G, Ye F. 2021. Destabilisation and stabilisation of anthocyanins in purple-fleshed sweet potatoes: A review. *Trends in Food Science & Technology*, **116**, 1141–1154.

Jaakola L. 2013. New insights into the regulation of anthocyanin biosynthesis in fruits. *Trends Plant Science*, **18**, 477–483.

Jaakola L, Määttä K, Pirttilä A M, Törrönen R, Kärenlampi S, Hohtola A. 2002. Expression of genes involved in anthocyanin biosynthesis in relation to anthocyanin, proanthocyanidin, and flavonol levels during bilberry fruit development. *Plant Physiology*, **130**, 729–739.

Jiang J, Huang H, Gao Q, Li Y, Xiang H, Zeng W, Xu L, Liu X, Li J, Mi Q, Deng L, Yang W, Zhang J, Yang G, Li X. 2023. Effects of editing *DFR* genes on flowers, leaves, and roots of tobacco. *BMC Plant Biology*, **23**, 349.

Johnson E T, Ryu S, Yi H, Shin B, Cheong H, Choi G. 2001. Alteration of a single amino acid changes the substrate specificity of dihydroflavonol 4-reductase. *Plant Journal*, **25**, 325–333.

Johnson E T, Yi H, Shin B, Oh B J, Cheong H, Choi G. 1999. *Cymbidium hybrida* dihydroflavonol 4-reductase does not efficiently reduce dihydrokaempferol to produce orange pelargonidin-type anthocyanins. *Plant Journal*, **19**, 81–85.

Kanehisa M, Goto S. 2000. KEGG: Kyoto Encyclopedia of Genes and Genomes. *Nucleic Acids Research*, **28**, 27–30.

Kapoor L, Simkin A J, Doss C G P, Siva R. 2022. Fruit ripening: dynamics and integrated analysis of carotenoids and anthocyanins. *BMC Plant Biology*, **22**,

Katsu K, Suzuki R, Tsuchiya W, Inagaki N, Yamazaki T, Hisano T, Yasui Y, Komori T, Koshio M, Kubota S, Walker A R, Furukawa K, Matsui K. 2017. A new buckwheat dihydroflavonol 4-reductase (DFR), with a unique substrate binding structure, has altered substrate specificity. *BMC Plant Biology*, **17**, 239.

Katsumoto Y, Fukuchi-Mizutani M, Fukui Y, Brugliera F, Holton T A, Karan M, Nakamura N, Yonekura-Sakakibara K, Togami J, Pigeaire A, Tao G Q, Nehra N S, Lu C Y, Dyson B K, Tsuda S, Ashikari T, Kusumi T, Mason J G, Tanaka Y. 2007. Engineering of the rose

flavonoid biosynthetic pathway successfully generated blue-hued flowers accumulating delphinidin. *Plant and Cell Physiology*, **48**, 1589–1600.
Koes R, Verweij W, Quattrocchio F. 2005. Flavonoids: a colorful model for the regulation and evolution of biochemical pathways. *Trends Plant Science*, **10**, 236–242.
Kubasek W L, Shirley B W, McKillop A, Goodman H M, Briggs W, Ausubel F M. 1992. Regulation of flavonoid biosynthetic genes in germinating *Arabidopsis* seedlings. *The Plant Cell*, **4**, 1229–1236.
Kumar S, Stecher G, Tamura K. 2016. MEGA7: Molecular Evolutionary Genetics Analysis Version 7.0 for bigger datasets. *Molecular Biology and Evolution*, **33**, 1870–1874.
Li C, Shi L, Li X, Wang Y, Bi Y, Li W, Ma H, Chen B, Zhu L, Fu Y. 2022. ECAP is a key negative regulator mediating different pathways to modulate salt stress-induced anthocyanin biosynthesis in *Arabidopsis*. *New Phytologist*, **233**, 2216–2231.
Liu H, Lou Q, Ma J, Su B, Gao Z, Liu Y. 2019. Cloning and functional characterization of dihydroflavonol 4-reductase gene involved in anthocyanidin biosynthesis of grape hyacinth. *International Journal of Molecular Sciences*, **20**,
Liu J, Ai X, Wang Y, Lu Q, Li T, Wu L, Sun L, Shen H. 2020. Fine mapping of the *Ca3GT* gene controlling anthocyanin biosynthesis in mature unripe fruit of *Capsicum annuum* L. *Theoretical and Applied Genetics*, **133**, 2729–2742.
Livak K J, Schmittgen T D. 2001. Analysis of relative gene expression data using real-time quantitative PCR and the $2^{-\Delta\Delta CT}$ method. *Methods*, **25**, 402–408.
Mattioli R, Francioso A, Mosca L, Silva P. 2020. Anthocyanins: A comprehensive review of their chemical properties and health effects on cardiovascular and neurodegenerative diseases. *Molecules*, **25**, E3809.
Mujanović I, Balijagić J, Bajagić M, Poštić D, Đurović S. 2024. Variations in polyphenol content and anthocyanin composition in bilberry populations (*Vaccinium myrtillus* L.) due to environmental factors. *Journal of Food Composition and Analysis*, **136**, 106732.
Nakatsuka T, Suzuki T, Harada K, Kobayashi Y, Dohra H, Ohno H. 2019. Floral organ- and temperature-dependent regulation of anthocyanin biosynthesis in *Cymbidium* hybrid flowers. *Plant Science*, **287**, 110173.
Petit P, Granier T, d'Estaintot B L, Manigand C, Bathany K, Schmitter J-M, Lauvergeat V, Hamdi S, Gallois B. 2007. Crystal structure of grape dihydroflavonol 4-reductase, a key enzyme in flavonoid biosynthesis. *Journal of Molecular Biology*, **368**, 1345–1357.
Petroni K, Pilu R, Tonelli C. 2014. Anthocyanins in corn: A wealth of genes for human health. *Planta*, **240**, 901–911.
Polashock J J, Griesbach R J, Sullivan R F, Vorsa N. 2002. Cloning of a cDNA encoding the cranberry dihydroflavonol-4-reductase (DFR) and expression in transgenic tobacco. *Plant Science*, **163**, 241–251.
Rodríguez-Lorenzo M, Mauri N, Royo C, Rambla J L, Diretto G, Demurtas O, Hilbert G, Renaud C, Tobar V, Huete J, Delrot S, Granell A, Martínez-Zapater J M, Carbonell-Bejerano P. 2023. The flavour of grape colour: anthocyanin content tunes aroma precursor composition by altering the berry microenvironment. *Journal of Experimental Botany*, **74**, 6369–6390.
Rodríguez-Mena A, Ochoa-Martínez L A, González-Herrera S M, Rutiaga-Quiñones O M, González-Laredo R F, Olmedilla-Alonso B. 2023. Natural pigments of plant origin: Classification, extraction and application in foods. *Food Chemistry*, **398**,
Ruan H, Shi X, Gao L, Rashid A, Li Y, Lei T, Dai X, Xia T, Wang Y. 2022. Functional analysis of the dihydroflavonol 4-reductase family of *Camellia sinensis*: exploiting key amino acids to reconstruct reduction activity. *Horticulture Research*, **9**, uhac098.
Saigo T, Wang T, Watanabe M, Tohge T. 2020. Diversity of anthocyanin and proanthocyanin biosynthesis in land plants. *Current Opinion In Plant Biology*, **55**, 93–99.
Seitz C, Vitten M, Steinbach P, Hartl S, Hirsche J, Rathje W, Treutter D, Forkmann G. 2007. Redirection of anthocyanin synthesis in *Osteospermum hybrida* by a two-enzyme manipulation strategy. *Phytochemistry*, **68**, 824–833.
Shi L, Li X, Fu Y, Li C. 2023. Environmental stimuli and phytohormones in anthocyanin biosynthesis: A comprehensive review. *International Journal of Molecular Sciences*, **24**, 16415.
Shi Q, Du J, Zhu D, Li X, Li X. 2020. Metabolomic and transcriptomic analyses of anthocyanin biosynthesis mechanisms in the color mutant *Ziziphus jujuba* cv. Tailihong. *Journal of Agricultural and Food Chemistry*, **68**, 15186–15198.
Sun C, Deng L, Du M, Zhao J, Chen Q, Huang T, Jiang H, Li C B, Li C. 2020. A transcriptional network promotes anthocyanin biosynthesis in tomato flesh. *Molecular Plant*, **13**, 42–58.
Sun H L, Wang X Y, Shang Y, Wang X Q, Du G D, LÜ D G. 2021. Preharvest application of melatonin induces anthocyanin accumulation and related gene upregulation in red pear (*Pyrus ussuriensis*). *Journal of Integrative Agriculture*, **20**, 2126–2137.
Tanaka Y, Brugliera F, Chandler S. 2009. Recent progress of flower colour modification by biotechnology. *International Journal of Molecular Sciences*, **10**, 5350–5369.
Tian J, Chen M C, Zhang J, Li K T, Song T T, Zhang X, Yao Y C. 2017. Characteristics of dihydroflavonol 4-reductase gene promoters from different leaf colored Malus crabapple cultivars. *Horticulture Research*, **4**, 17070.
Wan H, Yuan W, Ruan M, Ye Q, Wang R, Li Z, Zhou G, Yao Z, Zhao J, Liu S, Yang Y. 2011. Identification of reference genes for reverse transcription quantitative real-time PCR normalization in pepper (*Capsicum annuum* L.). *Biochemical and Biophysical Research Communications*, **416**, 24–30.
Wang G, Chen B, Du H, Zhang F, Zhang H, Wang Y, He H, Geng S, Zhang X. 2018. Genetic mapping of anthocyanin accumulation-related genes in pepper fruits using a combination of SLAF-seq and BSA. *PLoS ONE*, **13**, e0204690.
Wang X, Chen X, Luo S, Ma W, Li N, Zhang W, Tikunov Y, Xuan S, Zhao J, Wang Y, Zheng G, Yu P, Bai Y, Bovy A, Shen S. 2022. Discovery of a *DFR* gene that controls anthocyanin accumulation in the spiny *Solanum* group: roles of a natural promoter variant and alternative splicing. *Plant Journal*, **111**, 1096–1109.
Xia D, Zhou H, Wang Y, Li P, Fu P, Wu B, He Y. 2021. How rice organs are colored: The genetic basis of anthocyanin biosynthesis in rice. *The Crop Journal*, **9**, 598–608.
Xie D Y, Jackson L A, Cooper J D, Ferreira D, Paiva N L. 2004. Molecular and biochemical analysis of two cDNA clones encoding dihydroflavonol-4-reductase from *Medicago truncatula*. *Plant Physiology*, **134**, 979–994.
Xu H, Wang G, Ji X, Xiang K, Wang T, Zhang M, Shen G, Zhang R, Zhang J, Chen X. 2024. JrATHB-12 mediates JrMYB113 and JrMYB27 to control the anthocyanin levels in different types of red walnut. *Journal of Integrative Agriculture*, **23**, 2649–2661.
Ying J, Wen S, Cai Y, Ye Y, Li L, Qian R. 2024. Decoding anthocyanin biosynthesis regulation in *Asparagus officinalis* peel coloration: Insights from integrated metabolomic and transcriptomic analyses. *Plant Physiology and Biochemistry*, **215**, 108980.
Zhang J, Li S, An H, Zhang X, Zhou B. 2022. Integrated transcriptome and metabolome analysis reveals the anthocyanin biosynthesis mechanisms in blueberry (*Vaccinium corymbosum* L.) leaves under different light qualities. *Frontiers in Plant Science*, **13**, 1073332.
Zhang S L, Deng P, Xu Y C, Lü S W, Wang J Q. 2016. Quantification and analysis of anthocyanin and flavonoids compositions, and antioxidant activities in onions with three different colors. *Journal of Integrative Agriculture*, **15**, 2175–2181.
Zhang Y, Butelli E, Martin C. 2014. Engineering anthocyanin biosynthesis in plants. *Current Opinion in Plant Biology*, **19**, 81–90.
Zhou Y, Deng Y, Liu D, Wang H, Zhang X, Liu T, Wang J, Li Y, Ou L, Liu F, Zou X, Ouyang B, Li F. 2021. Promoting virus-induced gene silencing of pepper genes by a heterologous viral silencing suppressor. *Plant Biotechnology Journal*, **19**, 2398–2400.
Zhu L, Liao Y, Zhang T, Zeng Z, Wang J, Duan L, Chen X, Lin K, Liang X, Han Z, Huang Y, Wu W, Hu H, Xu Z F, Ni J. 2024. Reactive oxygen species act as the key signaling molecules mediating light-induced anthocyanin biosynthesis in Eucalyptus. *Plant Physiology and Biochemistry*, **212**, 108715.

Executive Editor-in-Chief Sanwen Huang
Managing Editor Lingyun Weng